Utilizing multiplets as an independent assessment of relative microseismic location uncertainty

Alex Hakso[1] and Mark Zoback[1]

Abstract

Location uncertainty is a key factor affecting interpretation of microseismic data associated with multistage hydraulic fracturing. We provide an independent assessment of relative microseismic event location uncertainty using multiplets — microseismic events that occur in essentially the same place with the same source characteristics. We establish a relationship between waveform similarity and hypocentral separation using synthetic events in a representative velocity model, finding an upper bound of 15 m between events in any given multiplet group. This implies that greater separation of locations for events within a multiplet reflects relative location error. We identified hundreds of multiplet groups in a case study in the Barnett with unusually high-quality data. All stages were recorded with two downhole monitoring arrays. Although the events within each multiplet group must be within 15 m of each other to produce nearly identical waveforms on the recording arrays, the scatter in contractor-provided event locations from the multiplet centroid is about 60 m for the most well-located multiplet events with source receiver distances of 150–200 m, despite a stated absolute location uncertainty of about 30 m. The scatter in event locations increases to 120 m when the source receiver distance is more than 250 m.

Introduction

Characterizing the nature and degree of absolute and relative event location uncertainty in microseismic data is necessary to ensure that interpretations are justified by the data. Contractor-reported uncertainties typically refer to relative location uncertainties introduced by errors in phase-arrival picks. These errors, generally based on residual misfits, are often underestimated due to the challenges presented by the geometric limitations of downhole receiver networks. Poor spatial coverage and closely spaced receivers can result in correlated errors being mistaken for well-constrained event locations. In addition, location uncertainties reported by contractors generally exclude errors attributable to velocity-model errors. Velocity errors are common in unconventional reservoirs, and velocity models often do not account for the intrinsic anisotropy of shale formations (Grechka and Yaskevich, 2013). Although velocity models can be better calibrated using all available perforation shots, in the case study presented here, the velocity model was adjusted between stages to better locate the perforation shots. While this approach may be convenient for locating the events occurring within a given stage, it is not necessarily geologically reasonable.

Relative location error increases the scatter in located events, obscuring structural details and artificially increasing apparent affected reservoir volume. Error due to inaccurate arrival picks can be improved with template-matching techniques (Rutledge and Phillips, 2003; Song et al., 2010). In addition, a number of studies (Arrowsmith and Eisner, 2006; Grechka et al., 2016; Eaton, 2017) have utilized the double-difference method (Waldhauser and Ellsworth, 2000) to reduce relative location error to identify features such as faults. Kocon and van der Baan (2012) utilized the double-difference algorithm in a heavy oil field with multiple downhole monitoring arrays. Kocon and van der Baan's analysis suggested typical relative location uncertainties of approximately 40 m, with 1.7% of events mislocated by up to several hundred meters. While the double-difference algorithm has the advantage of reducing the impact of uncertainties in the velocity model, thus obtaining more precise relative locations, it can only be used when there are three or more recording arrays available (Hurd, 2012). In this paper, we use multiplets — earthquakes that originate in nearly the same place and share source characteristics — to provide an independent assessment of the reliability of microseismic event relative locations and illustrate the process with a case study in the Barnett. A synthetic analysis was carried out to confirm relative location constraints.

Multiplets have been observed in both natural and fluid-injection environments (Poupinet et al., 1984; Moriya et al., 1994). In hydraulic fracturing, monotonically increasing fluid pressure (and thus reducing effective normal stress) on fractures throughout stimulation of a stage produces an environment conducive to repeated slip events, which can be identified through their waveform similarity. Following Stein and Wysession (2003), a waveform, $u(t)$, is represented in the time domain as:

$$u(t) = x(t) * e(t) * q(t) * i(t) \quad (1)$$

and

$$g(t) = e(t) * q(t), \quad (2)$$

where $x(t)$ is the source function, $i(t)$ is the instrument response, and $e(t)$ and $q(t)$ describe impedance contrasts and anelastic attenuation in the earth structure, respectively. Together, the earth-structure components make up the Green's function, which describes path effects. Given the earth's complex impedance and attenuation structure, each receiver has a unique Green's function associated with each source point in space. Similarly, the source function, as determined by the orientation of the slipping fault and nature of the slip, imposes a distinct signature on the radiated energy. Given the sensitivity of waveform character to location, fault orientation, and sense of slip, events with very similar waveforms have been interpreted as repeated ruptures of a fault or nearby parallel faults (Arrowsmith and Eisner, 2006).

An example multiplet group made up of 27 events from the case study discussed later is shown in Figure 1. The centroid of this multiplet is 185 m from the reference receiver. Both P- and S-phase arrivals are shown, with a high degree of similarity shown

[1]Stanford University.

https://doi.org/10.1190/tle36100829.1.

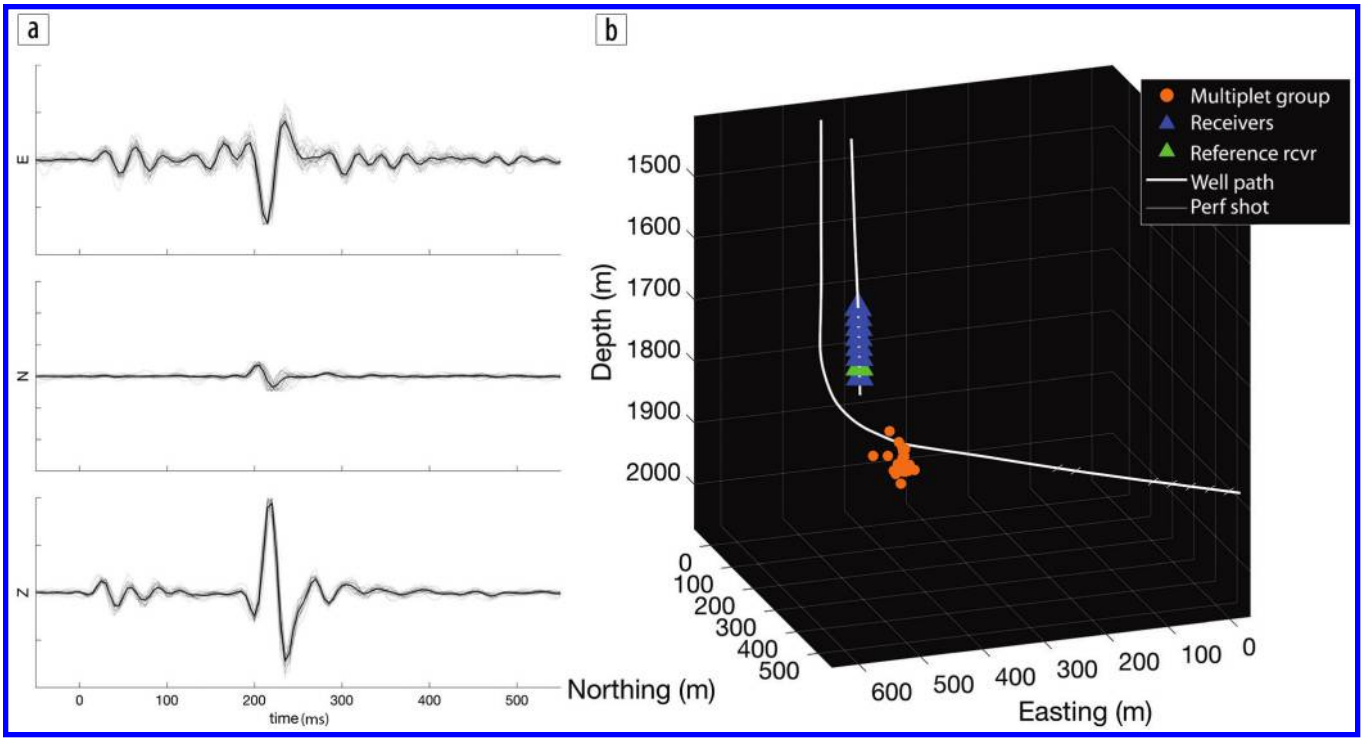

Figure 1. (a) Arrivals from a multiplet group of 27 events are superimposed, with the stacked trace bolded. (b) Contractor locations. The trace amplitudes are normalized, with scaling factors ranging across a factor of five with respect to the median amplitude, although nearly all are scaled by less than a factor of two.

on the high-amplitude components. Waveform similarity is consistent across the array.

The magnitude of scatter in microearthquake hypocenters within a multiplet is of particular interest in this study. Events that produce essentially identical seismograms must not only represent the same source, $x(t)$, but the same Green's function, $g(t)$, as well. Geller and Mueller (1980) suggest that for this to be the case the events must be separated by no more than $\lambda/4$, where λ represents the dominant wavelength of the seismic signal. In a hydraulic fracturing context, much of the radiated microseismic energy is above 200 Hz with shear-wave speeds of about 2.5 km/s. Therefore, the so-called quarter-wavelength hypothesis constrains event hypocenters to within a few meters of each other. Evaluating this hypothesis empirically, Thorbjarnardottir and Pechmann (1987) performed an experiment using mine blasts with known locations. Their results showed that similarity between seismograms of two different events is indeed a strong function of their source separation distance. They further found that the likelihood of false positives is low relative to the likelihood of false negatives. That is, events separated by more than $\lambda/4$ with similar waveforms are rare, while events within $\lambda/4$ that fail to display waveform similarity are relatively common. False positives did occur, however, prompting them to characterize the quarter-wavelength hypothesis as a "rough rule."

A number of authors have assembled empirical coherency functions for earthquakes with epicentral distances of tens of kilometers recorded on surface arrays (Abrahamson et al., 1991; Imtiaz et al., 2015). These studies demonstrate coherency breakdown well within a quarter wavelength of separation. Limited borehole observations (Vernon et al., 1991) indicate, however, that much of the signal distortion occurs in the top 150 m. The degradation of waveform similarity with hypocentral separation in borehole recordings at high frequency and short monitoring distance has not been adequately examined. We address the coherency-distance relationship in this context.

Relative location constraint

To better quantify the sensitivity of waveform similarity to earthquake origin distance, we carry out an analysis using the waveform forward-modeling tool fk3.2 (Zhu, 2014). The modeling method employed by fk3.2 utilizes the Thompson-Haskell propagator matrix technique, documented in Zhu and Rivera (2002). The software performs a double integral over wave numbers and frequencies and is capable of efficiently simulating many events in an elastic velocity model with many layers and high frequencies. While the software can simulate any focal mechanism, we utilize pure double-couple sources, specifying rupture properties appropriate for the microseismic context. Attenuation and conversion between phases at interfaces are included in the model, which is valuable for capturing waveform complexity.

We forward model and compare event waveforms with increasing hypocentral distance and observe the breakdown in coherency of the arrivals. Here, coherence is defined as the normalized crosscorrelation value of the arrival averaged across each component, weighted by the signal-to-noise ratio on each component.

The simulation geometry is shown in Figure 2. Each gray square in the figure represents a patch of 2500 sources with 1 m spacing. This cloud of microseismic events is nearly 1 km in width, with 22,500 unique events. The white well trajectories and colored receivers correspond with the geometry in the Barnett case study discussed later. For each pair of events assessed for waveform similarity, the focal mechanism is identical. We use the layered velocity model provided for the data set in hand. Likewise, the simulated spatial distribution of events is representative of the

case study microseismicity. The azimuth of the plane of simulated event hypocenters is arbitrary, as the Green's function is azimuthally invariant in this simplified, layered velocity model.

We find that the relationship between coherency degradation and increasing hypocentral distance is highly sensitive to the location of the source and receiver within the model, as well as the source-receiver distance. As the objective is to establish a relative location constraint applicable to the whole reservoir space, we simulate events across all distances and depths present in the data, comprising hundreds of millions of event pairs. Waveform similarity values are calculated for each event pair, and the values are binned by hypocentral separation. We observe a consistent relationship between hypocentral separation and waveform similarity, which gives the expected similarity value for two events with identical focal mechanisms (Figure A1). Additional details of the synthetic methodology are described in the Appendix.

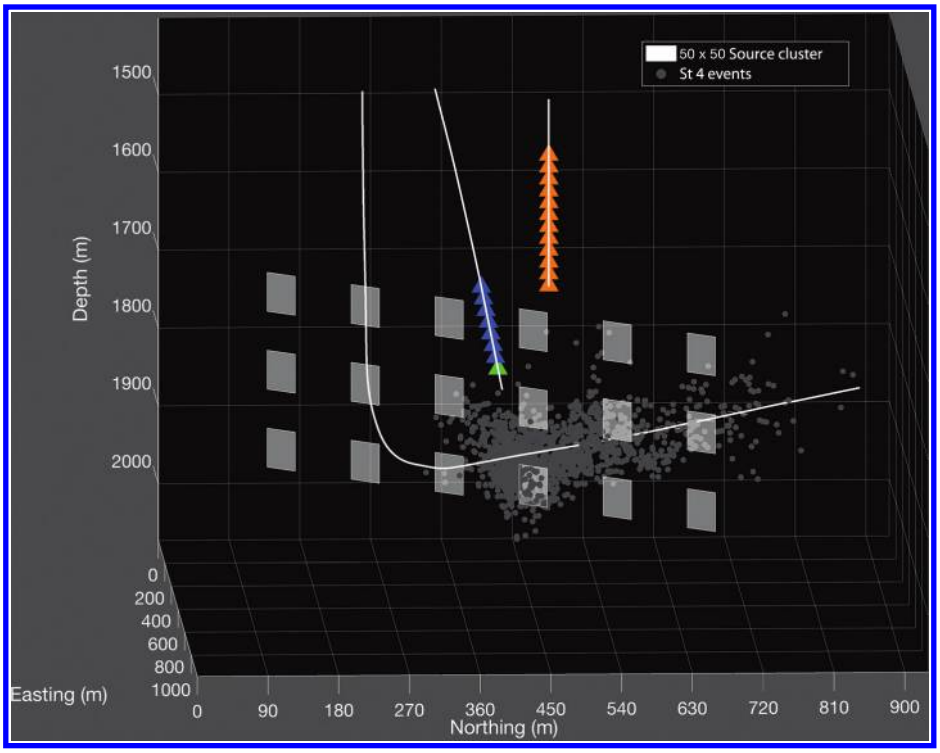

Figure 2. Synthetic source coverage. Reference receiver is in green.

The most relevant metric produced by the synthetic analysis is the probability of events separated by more than $\lambda/4$ exhibiting high waveform similarity. We calculate this probability for several similarity thresholds across a range of hypocentral separation values. In the literature, similarity thresholds distinguishing multiplets from repeating events range from 0.68 in Moriya et al. (2003) to 0.9 in many studies (e.g., Poupinet et al., 2008). A higher similarity threshold trades off an increase in false negatives for a reduction in false positives. Figure 3 shows the relationship between exceedance probability and hypocentral separation for a similarity threshold of 0.9. Note that even events with small hypocentral separations have a significant chance of falling below the similarity threshold. This suggests that the probability of categorizing nearly colocated events as dissimilar is relatively high, while the probability of categorizing two events separated by a significant distance as nearly colocated is very low. In short, the risk of false negatives is high (we may fail to identify some events that could be included in a group of multiplets), while the risk of false positives is low (events that are not part of the multiplet group are rejected). This result agrees with the Thorbjarnardottir and Pechmann (1987) experiments mentioned earlier and gives a high level of confidence for events identified as multiplets. Events separated by 15 m approach a four-sigma confidence level of remaining below the similarity threshold, while events separated by more than 15 m are yet less likely to randomly exceed the 0.9 similarity threshold. Thus, a threshold of 0.9 provides an acceptably low false-positive rate while constraining identified multiplets to within 15 m. Although this constraint allows for greater separation than the quarter-wavelength rule of thumb (which suggests an approximately 5 m constraint), the 15 m bound is sufficiently conservative for several reasons, enumerated in the Appendix.

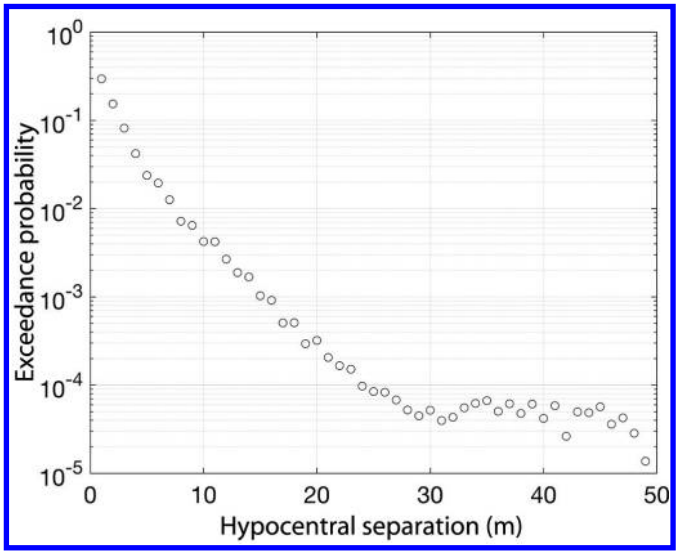

Figure 3. A 0.90 normalized crosscorrelation threshold gives a rapidly decreasing exceedance probability with hypocentral separation.

Barnett case study

Taking advantage of the relative location constraint of microseismic events within multiplet groups established by the synthetic analysis, we carry out a multiplet analysis of a microseismic data set acquired during hydraulic fracturing operations in the Barnett Shale in the Fort Worth Basin. The data set we utilized in this analysis involved a total of 20 three-component geophones sampling at 1 ms intervals deployed in two downhole arrays that were used to monitor hydraulic fracturing operations in three parallel horizontal wells. The arrays were repositioned four times in five wells throughout the hydraulic fracturing process to minimize the distance between the microseismic events and the receivers,

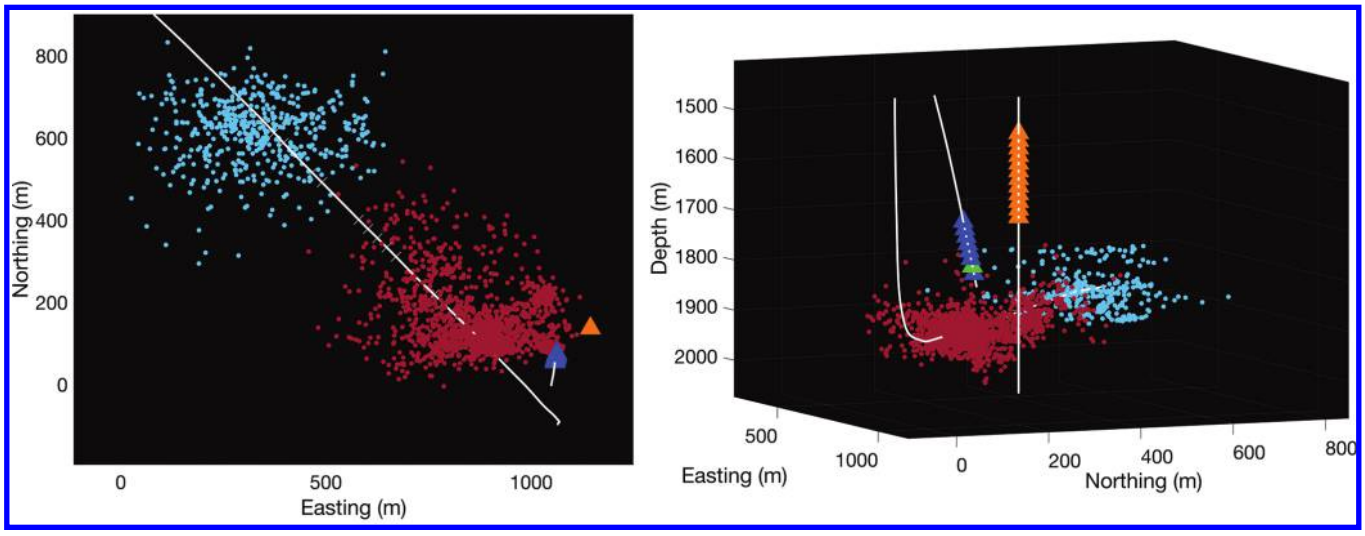

Figure 4. Map and perspective views of microseismic events recorded during stages 3 (light blue dots) and 4 (red dots) on two vertical arrays (orange and blue triangles).

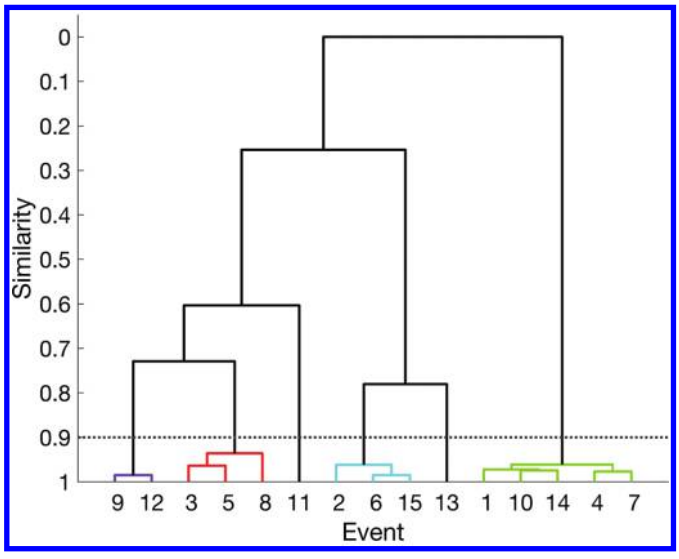

Figure 5. This schematic dendrogram demonstrates the increasing number of groups formed as the similarity requirement is relaxed.

providing an unusually favorable monitoring geometry throughout the hydraulic fracturing operation. The maximum distance between an event and the nearest tool is approximately 1000 m. The velocity model used by the microseismic service company was initially derived from sonic-log data. To adjust for potential velocity changes induced by the hydraulic fracturing operation, perforation shots for each of the five hydraulic fracturing stages in the well being studied were used to calibrate and update the velocity model. Using the calibrated velocity model, the average error when relocating the perforation shots was approximately 30 m, which the contractor used as a proxy for event location uncertainty.

More than 26,000 microseismic events were detected during the stimulation, with approximately 5000 locations provided by the contractor. The data used in this study are associated with the first well stimulated in the region, so the reservoir had not been perturbed by hydraulic operations in nearby wells. The operational geometry is displayed in Figure 4, along with events associated with stages 3 and 4, recorded on two vertical arrays shown by orange and blue triangles. These stages allow us to analyze events over a range of monitoring distances, with a consistent recording geometry and a previously unperturbed reservoir between the events and the receiver arrays.

Multiplet identification. A match filter with shear-wave templates enables rapid, effective identification of similar waveforms. After initial processing to remove various sources of noise, we employed a third-order, zero-phase Butterworth band-pass filter from 20 to 200 Hz to suppress frequencies outside the pass band without introducing a frequency-dependent delay to the signal. The wide pass band allows subtleties in the Green's function to be preserved in the waveforms. Targeting prominent arrivals, we select template events using a graphical user interface. These templates are crosscorrelated on each component of a reference receiver with all available data. The crosscorrelation scheme is adapted from a MATLAB script written by Padfield (2012), which is itself an adaptation of a preexisting 2D crosscorrelation MATLAB function. The process produces pairwise maximum similarity values between 0 and 1 for each event and each template.

Event clustering. To this point, the similarity analysis is carried out in a pairwise fashion, while multiplets can involve multiple microearthquakes. There are various methodologies for clustering similar events into physically meaningful groups (Aster and Scott, 1993). An "open-tree" or "breadth-first" algorithm requires only that each event is highly correlated with at least one other event in the group. With many events, it is possible for extended similarity chains to eventually connect events that are dissimilar. This could be especially problematic in the high-event-density context of a hydraulic fracturing operation. A "closed-tree" approach requires that each event in a cluster is highly correlated with each other event. As demonstrated by Thorbjarnardottir and Pechmann (1987) and observed in our synthetic analysis, the frequency of false negatives is such that this approach produces artificially small multiplet groups. We have used an agglomerative hierarchical clustering similar to that used by Rowe et al. (2002), which is well suited to addressing the shortcomings of both open-tree and closed-tree methodologies. It allows us to account for the varying significance of the similarity measures on each geophone component, based on their signal-to-noise ratio. It also allows for

fine-grained adjustments to group similarity calculation methods and tuning for closure considerations, which is crucial for returning physically meaningful results.

Further exploration of the appropriate threshold is aided by the nature of the clustering algorithm, which produces groups at all similarity levels. Sensitivity of the clustering results to the imposed similarity threshold is easily visualized in the dendrogram produced by the algorithm and is displayed schematically in Figure 5. In this figure, a similarity threshold of 0.9 produces four multiplet groups. A threshold of 0.75 would merge event 13 into the teal-colored group, and a threshold of 0.7 would merge the purple and red groups. Clearly delineated groups are unaffected by minor threshold changes. Those that are less clearly delineated are manually inspected. In agreement with the synthetic case, we enforce an average normalized crosscorrelation coefficient threshold of 0.9 to confidently categorize events as occurring within 15 m of each other.

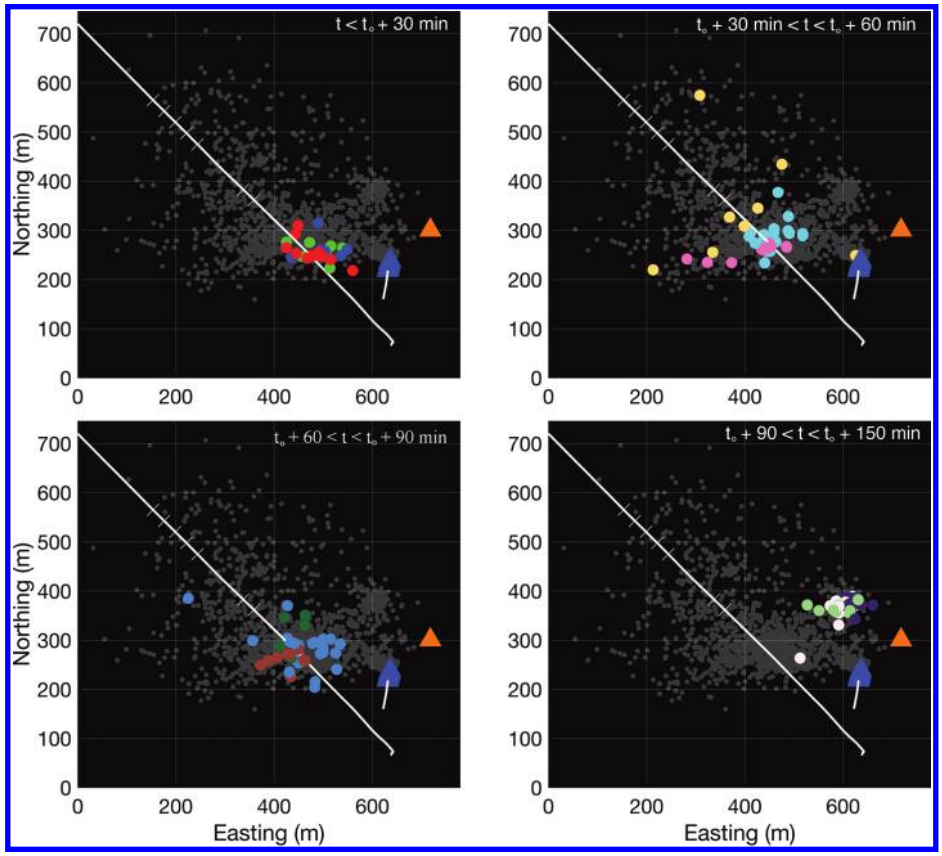

Figure 6. Select multiplet groups recorded during stage 4 are displayed in order of increasing time of the first event in the multiplet group. The time range with respect to the onset of pumping t_o is given, and each color represents a group. The groups overlay all contractor locations of microseismic events in the stage (light gray). The intragroup scatter in reported locations ranges from ~75 to 200 m.

Multiplet group results. An analysis of nearly 10,000 events in two stages of hydraulic fracturing identified 202 multiplet groups distributed throughout the seismically active zone, ranging from two to 29 member events. Repeating events represent a significant portion of the total events, approximately 2% and 10% of stages 3 and 4, respectively. Since stage 3 is significantly farther from the receiver array than stage 4, the difference in proportion of events that are identified as multiplets is likely due to the role of noise dramatically increasing the rate of false negatives. As can be seen in Figure 6, which displays multiplet groups with seven or more members from stage 4, the repeating events occur over much of the seismically active region in the stage. Approximately three-quarters of multiplet groups consist of two or three events.

To ensure that the multiplet identification procedure is not producing false positives due to noise, we selected a reference receiver farther from the stimulation zone, repeating the analysis in this lower signal-to-noise environment. Here, a subset of the multiplets identified in the original analysis was identified, and no new events were included. This confirms that independent events are not being mistakenly identified as multiplets in noisy signals.

Relative locations of microseismic events. Recall that the conservative hypocentral separation bound provided by the synthetic analysis constrains multiplet hypocenters to within 15 m of each other, while the quarter-wavelength hypothesis suggests an upper bound of about 5 m. Here, we see that the location scatter reflected in the contractor locations meaningfully exceeds both bounds. The contractor-provided event locations in the group of five multiplets displayed in Figure 7 span more than 250 m, despite the remarkable waveform similarity throughout the P- and S-arrivals, including codas. These events occurred in the same 20-minute window, beginning roughly an hour after the stage stimulation began.

Knowing that microseismic events within a multiplet group must be located in close proximity to each other, the location scatter is a measure of relative location uncertainty. As shown in Figure 8, multiplet groups farther from the receiver arrays show more scatter, indicating greater location uncertainty. Looking across all multiplet groups, median distance between each event and the centroid of its multiplet cluster is approximately 45 m. For doublets, this is an average event separation of 90 m. While the multiplet analysis cannot assess the quality of the absolute location for any given event, the magnitude of the scatter suggests that estimated uncertainties of 30 m determined by perforation shot relocations significantly overstate the reliability of the event locations.

Conclusion

Despite a favorable monitoring geometry, contractor event locations in the considered data set show significantly more scatter within multiplet groups than estimated using routine microearthquake location techniques. Our synthetic analysis demonstrates that the scatter is largely artificial and that uncertainties inferred

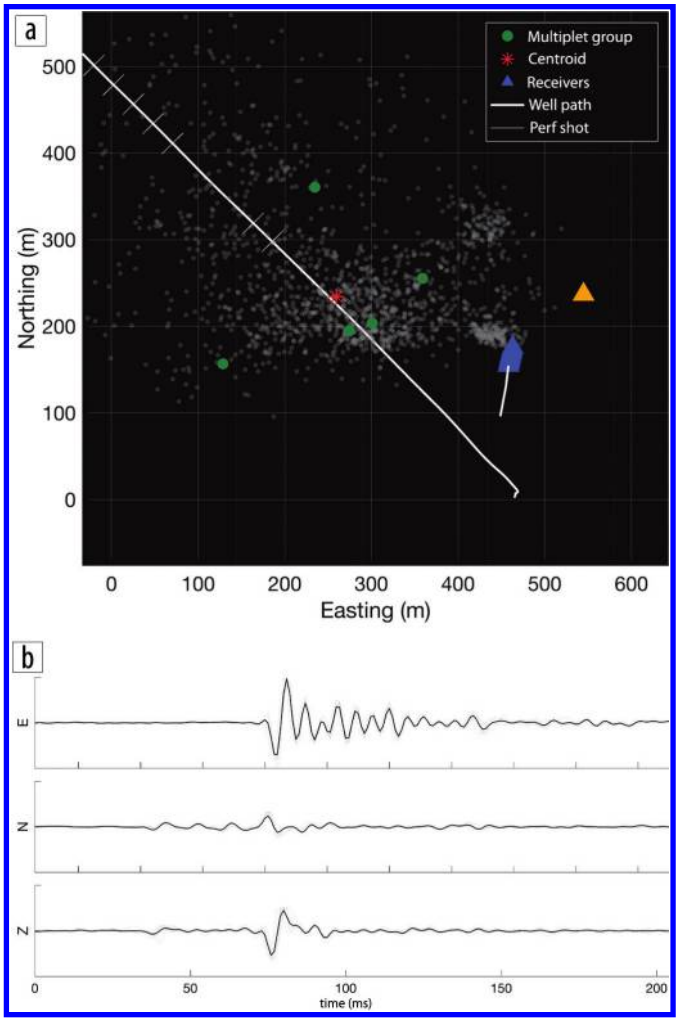

Figure 7. (a) Five located multiplet events occurring during the stimulation of stage 5 are plotted, superposed on all contractor locations of microseismic events in the stage (light gray). (b) Their superimposed waveforms, displaying similarity on all components from shear-wave onset into the coda. The amplitudes are normalized, with a maximum scaling factor of 1.65 times the median amplitude event.

by perforation shot relocations mischaracterize the reliability of the event locations. The presented multiplet identification technique is effective for providing independent insight into location uncertainty of microseismic events, ensuring that interpretations of event locations are commensurate with their quality. Our synthetic analysis provides an upper bound of 15 m on hypocentral separation between events in a multiplet group. This bound is somewhat looser than implied by the quarter-wavelength estimate, which is unsurprising given the conservative approach we took in our synthetic analysis. As the synthetic analysis is carried out in a manner representative of many hydraulically fractured reservoirs, we believe this bound is generally applicable for multiplets recorded with downhole microseismic monitoring with similar monitoring distances. When applying this bound to other data sets, it should be noted that the bound is dependent on frequency content, geologic complexity, and source-receiver distance; larger source-receiver distances, more homogenous geology, or lower frequencies might loosen this constraint still further. TLE

Acknowledgments

The authors would like to thank Total E&P for providing the case study data, a Chevron Fellowship, and Jim Rutledge for instructive, thorough feedback.

Corresponding author: ahakso@stanford.edu

References

Abrahamson, N. A., J. F. Schneider, and J. C. Stepp, 1991, Empirical spatial coherency functions for application to soil-structure interaction analyses: Earthquake Spectra, **7**, no. 1, 1–27, https://doi.org/10.1193/1.1585610.

Arrowsmith, S. J., and L. Eisner, 2006, A technique for identifying microseismic multiplets and application to the Valhall Field, North Sea: Geophysics, **71**, no. 2, V31–V40, https://doi.org/10.1190/1.2187804.

Aster, R. C., and J. Scott, 1993, Comprehensive characterization of waveform similarity in microearthquake data sets: Bulletin of the

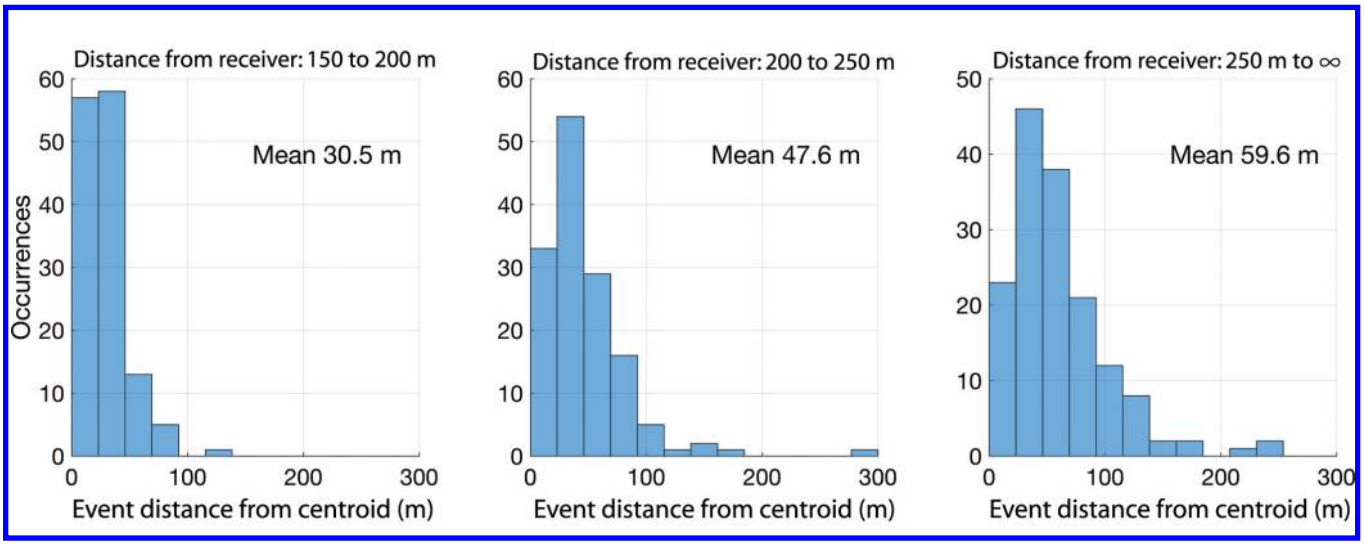

Figure 8. Distribution of event distance from the multiplet centroid, as per contractor locations. Each panel corresponds with a different source receiver distance bin, with distance to reference receiver increasing from left to right.

Seismological Society of America, **83**, no. 4, 1307–1314, http://www.bssaonline.org/content/83/4/1307.short, accessed 15 August 2017.

Eaton, D., 2017, Dynamics of fault activation by hydraulic fracturing in overpressured shales: 79th Conference and Exhibition, EAGE, Extended Abstracts, https://doi.org/10.3997/2214-4609.201701672.

Geller, R. J., and C. S. Mueller, 1980, Four similar earthquakes in central California: Geophysical Research Letters, **7**, no. 10, 821–824, https://doi.org/10.1029/GL007i010p00821.

Grechka, V., Z. Li, and B. Howell, 2016, Relative location of microseismic events with multiple masters: Geophysics, **81**, no. 4, KS149–KS158, https://doi.org/10.1190/geo2015-0445.1.

Grechka, V., and S. Yaskevich, 2013, Azimuthal anisotropy in microseismic monitoring: A Bakken case study: Geophysics, **79**, no. 1, KS1–KS12, https://doi.org/10.1190/geo2013-0211.1.

Hurd, O., 2012, Geomechanical analysis of intraplate earthquakes and earthquakes induced during stimulation of low permeability gas reservoirs: PhD thesis, Stanford University.

Imtiaz, A., C. Cornou, P.-Y. Bard, and A. Zerva, 2015, Spatial coherence of seismic ground motion and geometric structure of the sub-surface: An example in Argostoli, Greece: Presented at 9th Colloque National AFPS 2015.

Kocon, K., and M. van der Baan, 2012, Quality assessment of microseismic event locations and traveltime picks using a multiplet analysis: The Leading Edge, **31**, no. 11, 1330–1337, https://doi.org/10.1190/tle31111330.1.

Moriya, H., K. Nagano, and H. Niitsuma, 1994, Precise source location of AE doublets by spectral matrix analysis of triaxial hodogram: Geophysics, **59**, no. 1, 36–45, https://doi.org/10.1190/1.1443532.

Moriya, H., H. Niitsuma, and R. Baria, 2003, Multiplet-clustering analysis reveals structural details within the seismic cloud at the Soultz geothermal field, France: Bulletin of the Seismological Society of America, **93**, no. 4, 1606–1620, https://doi.org/10.1785/0120020072.

Padfield, D., 2012, Generalized normalized cross correlation, normxcorr2_general: MATLAB File Exchange, http://www.mathworks.com/matlabcentral/fileexchange/29005-generalized-normalized-cross-correlation/content/normxcorr2_general.m, accessed 22 August 2017.

Poupinet, G., W. L. Ellsworth, and J. Frechet, 1984, Monitoring velocity variations in the crust using earthquake doublets: An application to the Calaveras Fault, California: Journal of Geophysical Research, **89**, no. B7, 5719–5731, https://doi.org/10.1029/JB089iB07p05719.

Poupinet, G., J. L. Got, and F. Brenguier, 2008, Monitoring temporal variations of physical properties in the crust by

Appendix

To establish an upper bound on the hypocentral separation between events in a multiplet group, we carry out a synthetic analysis. By simulating events separated by a range of distances, we establish a relationship between hypocentral separation distance and waveform similarity in our velocity model for events with identical strike, dip, and rake. This relationship is a function of the velocity model and the sampled range of source-receiver distances. The velocity model is a determining factor because, while the independent variable of interest is event separation, the response variable is determined in part by the Green's function; for events with a fixed separation distance, the Green's function varies as a function of the location of the sources and receiver in the velocity model. Therefore, any given source separation distance is associated with a distribution of coherence values, dependent on the location of the sources and receiver in the velocity model. This dependence introduces statistical noise in the relationship between event separation and coherence. To capture the distribution of coherence values for hypocentral separation, we calculate the coherence of hundreds of millions of event pairs. The mean of the distribution for each distance is given in Figure A1. More importantly, developing the distribution of similarity values allows for calculation of a relationship between a similarity threshold and probability of exceedance for a given hypocentral separation. The similarity-value threshold and the probability of misclassifying distant events as multiplets have an inverse relationship. To ensure selection of an appropriate similarity threshold for the microseismic context, we place our events in the contractor-provided reservoir velocity model and simulate events at a range of source-distances spanning those present in the case study, as shown in Figure 2.

In this experiment, we expect waveform coherency to break down more slowly than in the real earth for several reasons. First, the model does not contain scatterers, which produce significant sensitivity with respect to location in the behavior of the Green's function. Second, the velocity model is a layer-cake model, ignoring complexity introduced by dipping layers and 3D variation. Third, in this model, the source mechanism of each event is identical; real-world events that are not colocated in the earth are unlikely to occur on fault patches with identical strike, rake, and dip. Finally, this model neglects the effect of noise, which significantly reduces coherence in the waveforms. Accordingly, the bound identified by this analysis should be considered a conservative upper bound on interevent separation.

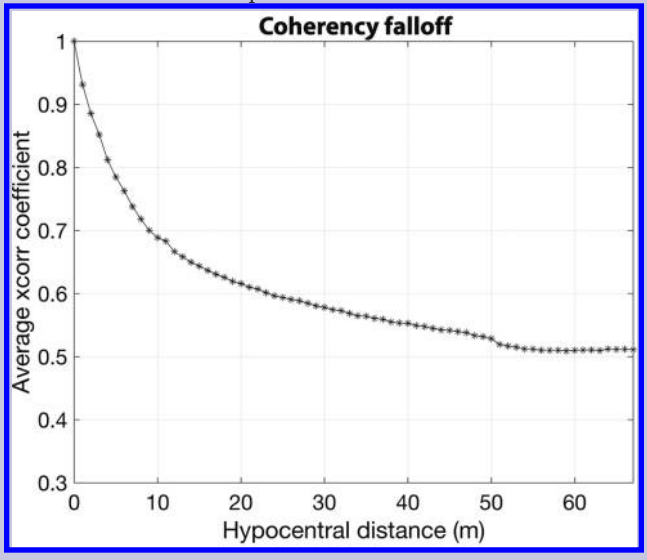

Figure A1. The expected value of the normalized crosscorrelation coefficient drops rapidly with the first 10 m of hypocentral separation.

cross-correlating the waveforms of seismic doublets: Advances in Geophysics, **50**, 373–399, https://doi.org/10.1016/S0065-2687(08)00014-9.
Rowe, C. A., R. C. Aster, B. Borchers, and C. J. Young, 2002, An automatic, adaptive algorithm for refining phase picks in large seismic data sets: Bulletin of the Seismological Society of America, **92**, no. 5, 1660–1674, https://doi.org/10.1785/0120010224.
Rutledge, J. T., and W. S. Phillips, 2003, Hydraulic stimulation of natural fractures as revealed by induced microearthquakes, Carthage Cotton Valley gas field, east Texas: Geophysics, **68**, no. 2, 441–452, https://doi.org/10.1190/1.1567214.
Song, F., H. S. Kuleli, M. N. Toksöz, E. Ay, and H. Zhang, 2010, An improved method for hydrofracture-induced microseismic event detection and phase picking: Geophysics, **75**, no. 6, A47–A52, https://doi.org/10.1190/1.3484716.
Stein, S., and M. Wysession, 2003, An introduction to seismology, earthquakes, and earth structure: John Wiley & Sons.
Thorbjarnardottir, B., and J. Pechmann, 1987, Constraints on relative earthquake locations from cross-correlation of waveforms: Bulletin of the Seismological Society of America, **77**, no. 5, 1626–1634, http://www.bssaonline.org/content/77/5/1626.short.
Vernon, F. L., J. Fletcher, L. Carroll, A. Chave, and E. Sembera, 1991, Coherence of seismic body waves from local events as measured by a small-aperture array: Journal of Geophysical Research. Solid Earth, **96**, no. B7, 11981–11996, https://doi.org/10.1029/91JB00193.
Waldhauser, F., and W. L. Ellsworth, 2000, A double-difference earthquake location algorithm: Method and application to the Northern Hayward Fault, California: Bulletin of the Seismological Society of America, **90**, no. 6, 1353–1368, https://doi.org/10.1785/0120000006.
Zhu, L., 2014, fk3.2: Seismo Lab.
Zhu, L., and L. A. Rivera, 2002, A note on the dynamic and static displacements from a point source in multilayered media: Geophysical Journal International, **148**, no. 3, 619–627, https://doi.org/10.1046/j.1365-246X.2002.01610.x.